ACS APPLIED MATERIALS & INTERFACES

Research Article

www.acsami.org

Activable Cell-Penetrating Peptide Conjugated Prodrug for Tumor Targeted Drug Delivery

Hong Cheng,[†] Jing-Yi Zhu,[†] Xiao-Ding Xu,[†] Wen-Xiu Qiu,[†] Qi Lei,[†] Kai Han,[†] Yin-Jia Cheng,[†] and Xian-Zheng Zhang*[,†,‡]

[†]Key Laboratory of Biomedical Polymers of Ministry of Education & Department of Chemistry and [‡]The Institute for Advanced Studies, Wuhan University, Wuhan 430072, P.R. China

Supporting Information

ABSTRACT: In this paper, an activable cell-penetrating peptide ($CR_8G_3PK_6$, ACPP) with a shielding group of 2,3-dimethylmaleic anhydride (DMA) was conjugated with antitumor drug doxorubicin (DOX) to construct a novel prodrug (DOX-ACPP-DMA) for tumor targeted drug delivery. The shielding group of DMA linked to the primary amines of K_6 through the amide bond was used to block the cell-penetrating function of the polycationic CPP (R_8) through intramolecular electrostatic attraction at physiological pH 7.4. At tumor extracellular pH 6.8, the hydrolysis of DMA led to charge reversal, activating the pristine function of CPP for improved cellular uptake by tumor cells. Confocal laser scanning microscopy (CLSM) and flow cytometry studies revealed that the cellular uptake of DOX-ACPP-DMA was significantly enhanced after acid-triggered activation in both HeLa and COS7 cells. After cell internalization, the overexpressed intracellular proteases would further trigger drug release in cells. Both in vitro and in vivo investigations showed that the peptidic prodrug exhibited significant tumor growth inhibition and demonstrated great potential for tumor therapy.

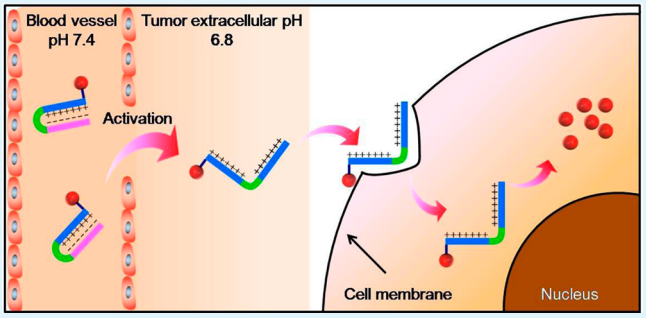

KEYWORDS: *cell-penetrating peptide, prodrug, cellular uptake, targeted drug delivery, tumor therapy*

1. INTRODUCTION

As an effective strategy for clinical tumor treatment, chemotherapy plays an important role in tumor suppressor and elimination.[1] However, most chemotherapy agents in the clinic have the deficiencies of high cytotoxicity, poor water-solubility, and nonselectivity, which seriously affects their curative effects.[2] Furthermore, although various amphiphilic block copolymers have widely been used for drug delivery, a number of issues, such as the premature drug leakage,[3] poor drug loading, and entrapment efficiency[4] have yet to be resolved. To solve these problems, over the past decade, researchers have proposed the concept of a prodrug, which has shown great potential in tumor treatment.[5,6] It should be noted that labile linkage was also introduced to prodrugs for stimuli-triggered drug release. However, it was found that the labile linkage was unable to maintain stability during circulation in vivo. As a result, the drug would be released to some extent before arriving in tumor tissues.[7−9]

In addition, cell-penetrating peptides (CPPs) were reported to have the ability to translocate antitumor drug into cells, and CPP-conjugated drugs have been used extensively for tumor therapy.[10−13] However, most CPPs are not cell specific, thus limiting their application in drug delivery. To address this challenge, researchers proposed an activable cell-penetrating peptide (ACPP) in which the CPP's cell-penetrating function is masked with an anionic peptide by a cleavable linker. Once in the tumor tissue, proteolysis of the linker would activate the cell-penetrating function of CPP.[14−17] However, it was also found that this type of ACPP is tumor-independent and most likely activated in the vasculature, which would influence its therapeutic effects.[18] It is known that the tumor microenvironment is weakly acidic (pH 5.7−7.0) compared to normal physiology (pH 7.4); thus, acid-sensitive shielding could be used to block the CPP's function. It was reported that amides with β-carboxylic acid groups are acid-sensitive.[19−23] For instance, 2,3-dimethylmaleic anhydride (DMA) could be attached to a primary amide stably under physiological conditions, whereas in a tumor acidic environment, the acid-labile amides would be hydrolyzed quickly.[24−27] Obviously, DMA could be used to construct acid-sensitive polyanionic inhibitory domains.

In this paper, an original ACPP ($CR_8G_3PK_6$) with a shielding group of DMA was conjugated with doxorubicin (DOX) through an amide bond to construct a novel prodrug DOX-ACPP-DMA for tumor targeted drug delivery. The ACPP consisted of a polycationic CPP, a tetrapeptide linker, and polylysines, which would become acid-sensitive polyanionic inhibitory domains after amidization by DMA. As shown in

Received: May 25, 2015
Accepted: July 10, 2015
Published: July 10, 2015

DOI: 10.1021/acsami.5b04517
ACS Appl. Mater. Interfaces 2015, 7, 16061−16069

Scheme 1. (A) Synthesis of Activable Cell-Penetrating Peptide Conjugated Prodrug (DOX-ACPP-DMA); (B) Structure Transformation of ACPP through Amidization of ACPP's Lysine Residues with DMA and its Acid-Triggered Hydrolysis; and (C) Schematic illustration of DOX-ACPP-DMA[a]

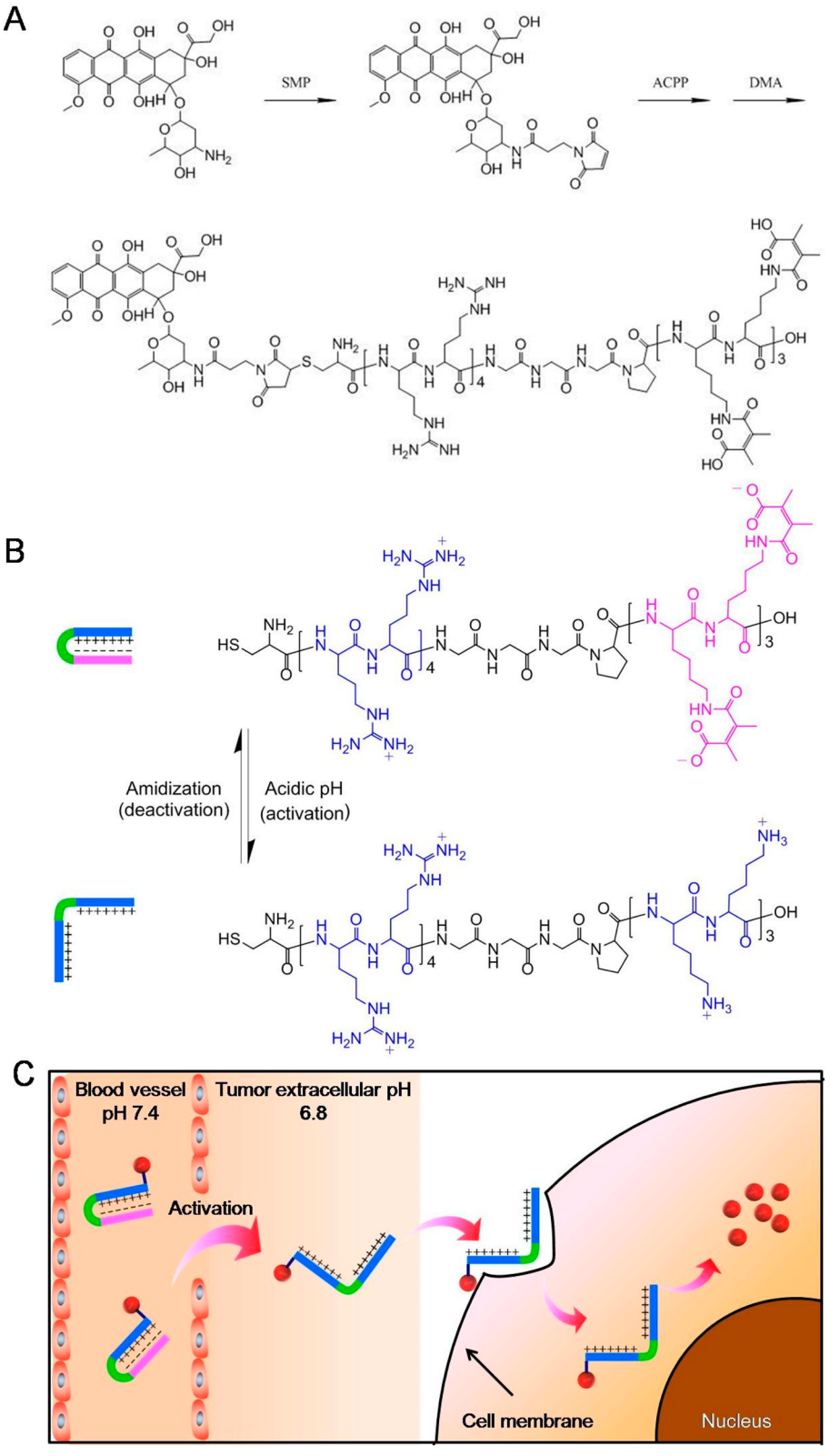

[a]Amidization of lysines' primary amines would inhibit the cell penetrating function of CPP (R_8), whereas acid-triggered hydrolysis would activate the primordial functioning CPP for fast cellular uptake by cells. Afterwards, the intracellular protease triggered the rapid release of DOX and demonstrated an efficient antitumor treatment in vivo. The red bullets represented DOX.

DOI: 10.1021/acsami.5b04517
ACS Appl. Mater. Interfaces 2015, 7, 16061−16069

Scheme 1, at physiological pH 7.4, DMA linked to the primary amines of K_6 could block the cell-penetrating function of the polycationic CPP (R_8) by intramolecular electrostatic attraction. Nevertheless, at tumor extracellular pH 6.8, the fast hydrolysis of DMA leads to charge reversal, activating the pristine function of CPP for fast cellular uptake by tumor cells. And after cell internalization, conjugated DOX release would be triggered effectively by the intracellular protease for tumor treatment.[28−31] The antitumor effect of DOX-ACPP-DMA both in vitro and in vivo is investigated in detail.

2. EXPERIMENTAL SECTION

2.1. Materials. 2-Chlorotrityl chloride resin (100−200 mesh; loading: 1.4 mmol/g), *N*-fluorenyl-9-methoxycarbonyl (Fmoc)-protected L-amino acids (Fmoc-Gly-OH, Fmoc-Pro-OH, Fmoc-Lys(Boc)-OH, Fmoc-Arg(Pdf)-OH, and Fmoc-Cys(Trt)-OH), *o*-benzotriazole-*N*,*N*,*N*′,*N*′-tetramethyluroniumhexafluorophosphate (HBTU), and peperidine were purchased from GL Biochem Ltd. (Shanghai, China) and used as received. Trifluoroacetic acid (TFA), triethylamine (TEA), diisopropylethylamine (DiEA), and *N*,*N*′-dimethylformamide (DMF) were obtained from Shanghai Reagent Chemical Co. (China) and distilled prior to use. Phenol, triisopropylsilane (TIS), 1,2-ethanedithiol (EDT), dichloromethane (DCM), methyl alcohol, and diethyl ether were provided by Shanghai Reagent Chemical Co. (China) and used directly. Doxorubicin hydrochloride (DOX·HCl) was purchased from Zhejiang Hisun Pharmaceutical Co. (China). Succinic anhydride (SA), *N*-succinimidyl 3-maleimidopropionate (SMP; >98%) was purchased from Zhejiang Jiaxing Biomatrix Co. Ltd. (China). 2,3-Dimethylmaleic anhydride (DMA) and fluorescamine were provided by Sigma-Aldrich (USA). Dulbecco's modified Eagle's medium (DMEM), 3-[4,5-dimethylthiazol-2-yl]-2,5-diphenyltetrazolium bromide (MTT), Hoechst 33342, fetal bovine serum (FBS), penicillin-streptomycin, trypsin, and Dulbecco's phosphate buffered saline (PBS) were obtained from GIBCO Invitrogen Corp. Cathepsin B (bovine spleen) was purchased from BiologyInstitute, Guangxi Academy of Sciences (China). All other reagents and solvents were of analytical grade and used without further purification.

2.2. Synthesis of ACPP. The peptide of ACPP ($CR_8G_3PK_6$) was synthesized manually on 2-chlorotrityl chloride resin via a standard Fmoc solid phase peptide synthesis (SPPS) method.[32] First, the resin was immersed in DMF and left standing to full swelling for 0.5 h. Then, the first amino acid coupling reaction was accomplished by adding a DMF-mixed solution of Fmoc-Lys (Boc)-OH (3 equiv, relative to resin loading) and DIEA (6 equiv) for 2 h at room temperature. However, all other coupling reactions were completed with Fmoc-protecting amino acid (4 equiv), HBTU (4 equiv), and DIEA (6 equiv) for 3 h at room temperature. In the progress of deprotection, 20% piperidine/DMF (v/v) was used to remove Fmoc-protected groups twice from the end of the peptide chain. These processes were repeated until all deprotection and acylation reactions were finished. Finally, the resin was washed with methyl alcohol and DCM three times, respectively, and dried under vacuum overnight. Peptide product was cleaved from the resin by adding the mixture of TFA, phenol, TIS, H_2O, and EDT in the volume ratio of 83:6.3:4.3:4.3:2.1 for 2 h. The resultant filtrate was concentrated by rotary evaporation and then precipitated in cold anhydrous diethyl ether. The crude product was separated from the solvent by centrifugation and dried under vacuum overnight. For the peptide to be purified further, it was dissolved in distilled water for lyophilization.

2.3. Synthesis of DOX-ACPP-DMA Conjugate. DOX was conjugated with the peptide by a linker of SMP. The synthesis of the DOX-SMP conjugate is shown in Scheme 1A. DOX, SMP, and TEA were dissolved in DMF and stirred for 3 h in the dark with a molar ratio of 1.1:1:2. The synthetic process was monitored by thin-layer chromatography (TLC, chloroform/methanol/ammonia = 70:30:3). The reaction solution was concentrated and precipitated in cold anhydrous diethyl ether. The product was collected by centrifugation and dried under vacuum for 24 h.

Then, DOX-ACPP was prepared by a Michael addition reaction between thiol and maleimide. Briefly, DOX-SMP and ACPP were dissolved in DMF with a molar ratio of 2:1. After stirring for 48 h, the reaction solution was transferred to a dialysis tube (MWCO 1000 Da) and then subjected to dialysis against 500 mL of DMF, which was replaced every 4 h to remove the unreacted DOX-SMP. After 48 h, the solution in the dialysis tube was concentrated and precipitated, and the product of DOX-ACPP was obtained using the same method described above.

Lastly, DOX-ACPP-DMA was prepared as follows: 3 equiv (to amino group) of DMA was added to the solution of DOX-ACPP, and the pH value was kept at ∼8.5 by adding 0.2 N NaOH dropwise. After 24 h, the solution was transferred to a dialysis tube (MWCO 1000 Da) and then subjected to dialysis against water at pH 8.5. The product of DOX-ACPP-DMA was obtained by freeze-drying. As a control, DOX-ACPP-SA was synthesized and purified using the same method.

2.4. Characterization of Various Conjugates. The molecular weight of ACPP, DOX-SMP, and DOX-ACPP was examined by electrospray ionization-mass spectrometry (ESI-MS) and matrix-assisted laser desorption ionization orthogonal time-of-flight mass spectrometry (MALDI-TOF-MS). DOX-ACPP-DMA was examined by ^{1}HNMR. Their purities were also examined by high-performance liquid chromatography (HPLC).

The zeta-potential changes of samples (0.25 mg/mL, 10 mM phosphate buffer solution (PBS)) at pH 6.8 and 7.4 were measured with a Nano-ZS ZEN3600 (Malvern Instruments). Each sample was measured at room temperature for 4 h.

Degradation of DMA in DOX-ACPP-DMA was measured by the fluorescamine method.[33,34] DOX-ACPP-DMA was incubated with PBS at pH 6.8 and 7.4. At specified times of 0, 10, 30, 60, 120, and 240 min, 1 mL of each sample was treated with 0.2 mL of fluorescamine solution in DMF (2 mg/mL) for 10 min at room temperature. Subsequently, the fluorescence intensity (F_s) was examined at an excitation wavelength of 365 nm and an emission wavelength of 475 nm by a fluorospectrophotometer. The fluorescence of blank PBS was considered to be F_c, and the fluorescence of the sample after the incubation in 0.1 M HCl for 24 h was defined as F_0 (100% of exposed amine). The hydrolysis effect of DMA was evaluated by the amount of exposed amine calculated by $(F_s - F_c)/(F_0 - F_c)\times 100\%$.

2.5. In Vitro Enzymatic Release of DOX. DOX in vitro release was performed by dialysis against PBS. The mixture of DOX-ACPP-DMA (3 mg) and 20 U cathepsin B was dispersed in 3 mL of 10 mM PBS buffer (pH 7.4) at 37 °C for 20 min. Afterwards, the solution was transferred to a dialysis tube (MWCO 1000 Da) and then subjected to dialysis against 10 mL of PBS (10 mM, pH 7.4) at 37 °C with constant shaking (200 rpm).[35] After hydrolysis by cathepsin B, the released DOX diffused outside the dialysis tube. During the progress, the whole medium was withdrawn for fluorescent measurements and replaced with 10 mL of fresh PBS at predetermined time intervals. The amount of DOX released was evaluated based on the fluorescence spectroscopy at an emission wavelength of 560 nm and an excitation wavelength of 470 nm. The release studies were carried out in triplicate, and the results shown are the averaged data.

2.6. Cell Culture. Human cervical carcinoma (HeLa) and transformed African green monkey SV40-transformed kidney fibroblast (COS7) cells were cultured in complete DMEM medium supplemented with 10% FBS and 1% antibiotic (penicillin-streptomycin, 10000 U/mL) at 37 °C in a humidified atmosphere containing 5% CO_2. All experiments were performed on cells in the logarithmic growth phase.

2.7. Cellular Uptake Evaluation by Confocal Laser Scanning Microscopy (CLSM). HeLa cells were seeded in 6-well plates and incubated in 1 mL of DMEM containing 10% FBS for 24 h at 37 °C. For cellular uptake observations, DOX-ACPP-DMA and DOX-ACPP-SA were added at an equivalent DOX concentration of 10 μg/mL, and the cells were incubated in fresh medium at pH 7.4 or 6.8, respectively, for another 1 h. Then, the nuclei of cells were counterstained with Hoechst 33342 for 15 min. The medium was then removed and

DOI: 10.1021/acsami.5b04517
ACS Appl. Mater. Interfaces 2015, 7, 16061−16069

washed six times with PBS, and fresh medium was added. The cellular uptake was observed under laser-scanning confocal microscopy (Nikon C1-si TE2000, Japan). As a control, COS7 cells were chosen to be incubated with DOX-ACPP-DMA by the same method.

To identify whether the DOX can be efficiently released from the conjugated prodrug, HeLa cells were incubated with DOX-ACPP-DMA at pH 6.8 for 2, 6, and 24 h, and the cells were then subjected to CLSM observations.

2.8. Cellular Uptake Quantitative Study by Flow Cytometry. HeLa cells were seeded onto a 6-well plate at a density of 1×10^5 cells/well in 1 mL of DMEM containing 10% FBS and cultured in a humidified 5% CO_2 atmosphere for 24 h. The original medium was replaced with DOX-ACPP-DMA and DOX-ACPP-SA containing DMEM at pH 7.4 and 6.8 with an equivalent DOX concentration of 10 μg/mL, respectively. After incubation for 1 h at 37 °C, HeLa cells were washed 3 times with PBS every 5 min. Thereafter, cells were harvested with trypsin, washed twice and resuspended in PBS, and centrifuged at 1000 rpm for 4 min at 4 °C. The supernatants were discarded, and the cell pellets were washed with PBS to remove the background fluorescence in the medium. After two cycles of washing and centrifugation, cells were resuspended with 200 μL of PBS. Cellular uptake of DOX conjugates was quantified using a FACS Calibur flow cytometer (BD Biosciences, USA). A minimum of 10,000 events per sample was analyzed. The fluorescence signal was analyzed in the PE channel, and the results were analyzed with Flow Jo software. As a control, COS7 cells were chosen to be incubated with DOX-ACPP-DMA for flow cytometry by the same method.

2.9. Cytotoxicity Assay. The in vitro cytotoxicities of DOX-ACPP-DMA against HeLa and COS7 cells were performed by MTT assay at pH 7.4 and 6.8, respectively. Briefly, HeLa or COS7 cells were seeded onto 96-well plates at a density of 6000 cells/well and incubated in 100 μL of DMEM containing 10% FBS for 24 h. Then, the original medium was replaced with DOX-ACPP-DMA containing DMEM at pH 7.4 and 6.8, respectively. After incubation for 4 h at 37 °C, the medium was replaced with 200 μL of fresh medium for another 44 h. Afterwards, MTT (5 mg/mL, 20 μL per well) was added, and the cells were incubated for another 4 h. Subsequently, the supernatant was removed, and 150 μL of DMSO was added to each well to dissolve the formazane of MTT. The optical density (OD) of each well was determined at 570 nm by a microplate reader (Bio-Rad, Model 550, USA). The relative cell viability was calculated according to the following equation: cell viability (%) = OD(sample)×100/OD(control), in which OD(control) was the optical density in the absence of sample, and OD(sample) was the optical density in the presence of sample. Each value was averaged from four independent experiments. As the control, the cytotoxicities of DOX, ACPP, and DOX-ACPP against HeLa cells were also performed by the same method.

2.10. In Vivo Antitumor Assay. Female KM mice (~4−5 weeks old) were obtained from the Wuhan University Animal Biosafety Level III Lab. All animal experiments were in accordance with the standard of the Experimental Animals Management Committee (Hubei Province, China) and approved by the Animal Research Committee of Zhongnan Hospital of Wuhan University (China). Hepatic tumor H22 cells extracted from abdominal dropsy were implanted onto the backs of the mice. The mice were supplied with sufficient food and water until the volume of the H22 tumor xenograft reached ~200 mm^3. The mice were then divided randomly into 4 groups with 5 mice in each group. First, as the negative group, mice were subcutaneously injected with PBS every day (PBS group). Concurrently, as the positive group, mice were injected subcutaneously with free DOX every day at a concentration of 5 mg of DOX per kg of mouse body weight (DOX group). Moreover, in the other two groups, mice were treated every day with DOX-ACPP-DMA (DOX-ACPP-DMA group) and DOX-ACPP-SA (DOX-ACPP-SA group), respectively, at an equivalent dose of 5 mg of DOX per kg of mouse body weight. During this process, the tumor volumes and weight of the mice were measured every day. The tumor volume was calculated as follows: $V = W^2L/2$, where W is the shortest diameter, and L is the longest diameter. After 14 days of treatment, the mice were sacrificed, and the major organs and tumors were collected for further analysis.

2.11. Histology Analysis. The major organs and tumors were fixed by 4% formalin, embedded in paraffin, and then sectioned. Sections with 7 μm thickness were mounted on glass slides and finally stained with hematoxylin/eosin and examined by light microscopy.

3. RESULTS AND DISCUSSION

3.1. Design, Synthesis, and Characterization of DOX-ACPP-DMA Conjugate. The conjugate designed for in vivo tumor targeted drug delivery should be stable to prolong the blood half-life and increase accumulation in the tumor site. This could be achieved by passivation of the conjugate with anionic groups, which would help reduce the zeta potential and provide a physical barrier between the blood components and negatively charged conjugates. After extravasation from the blood into the tumor site, it is also necessary for the conjugate to translocate the therapeutic payload across cellular membranes for cellular uptake.

As shown in Scheme 1A, a novel ACPP conjugated prodrug was designed for targeted drug delivery. First, an original peptide sequence ACPP (HS-$CR_8G_3PK_6$-COOH) was synthesized by the standard Fmoc solid phase peptide synthesis (SPPS) method, and the molecular weight found in the MALDI-TOF-MS spectrum was 2407 (calcd Mw: 2407) (Figure S1, Supporting Information (SI)). The purity of ACPP (91.8%) was examined by HPLC (Figure S2, SI). Meanwhile, the active ester group of SMP was used to react with DOX to obtain DOX-SMP. In the reaction, TEA was used to neutralize the hydrochloride salt and is favorable for DOX-SMP production. The molecular weight of DOX-SMP found in the ESI-MS spectrum was 717 $[M + Na]^+$ and 1411 $[2M + Na]^+$ (calcd Mw: 694) (Figure S3, SI). The purity of DOX-SMP (97.3%) was examined by HPLC (Figure S4, SI). Then, DOX-SMP was covalently attached to ACPP by a Michael addition to prepare the ACPP-conjugated prodrug. Its molecular weight found in the MALDI-TOF-MS spectrum was 3101 (calcd Mw: 3101) (Figure S5, SI). The purity of DOX-ACPP (92.7%) was examined by HPLC (Figure S6, SI).

Subsequently, the primary amines in K_6 residues were amidized to form acid-labile amides and reduce the zeta potential of ACPP. Before the modification of DMA, it was found that DOX-ACPP had a high zeta potential of 12.6 mV. After the modification, the zeta potential of DOX-ACPP-DMA changed to −21.3 mV, demonstrating the successful development of DOX-ACPP-DMA. Furthermore, the coupled DMA in DOX-ACPP-DMA was also characterized by ^{1}HNMR (Figure S7, SI). The main characteristic peak signals indicated the successful coupling of DMA to DOX-ACPP. The purity of DOX-ACPP-DMA (90.5%) was also examined by HPLC (Figure S8, SI). For demonstrating that DOX-ACPP-DMA had the charge conversion property under an acidic environment, as a control, DOX-ACPP-SA was synthesized by the same method except using SA instead of DMA, whose zeta potential was found to be −22.6 mV.

Under physiological conditions, ACPP would be inactive due to intramolecular electrostatic attraction (Scheme 1B), which would inhibit CPPs from interacting with cells. However, in the acidic tumor microenvironment, the fast hydrolysis of DMA led to charge reversal, activating the pristine function of CPP through the electrostatic repulsive force for fast cellular uptake by tumor cells. After cell internalization, the conjugated DOX

DOI: 10.1021/acsami.5b04517
ACS Appl. Mater. Interfaces 2015, 7, 16061−16069

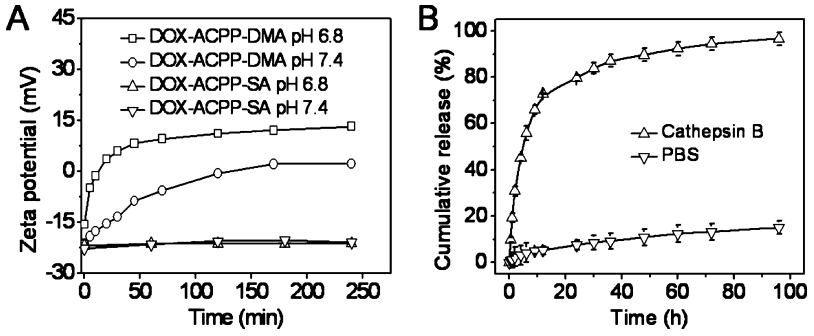

Figure 1. (A) Zeta potential changes of DOX-ACPP-DMA/SA exposed at pH 7.4 or 6.8 for different time periods. (B) In vitro drug release behavior of DOX-ACPP-DMA (1 mg/mL in pH 7.4 PBS) with the addition of 20 U cathepsin B at physiological temperature (37 °C).

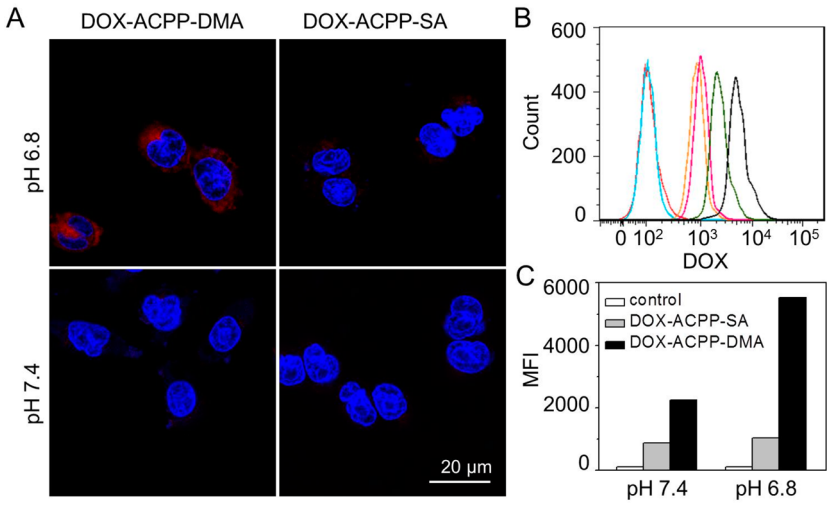

Figure 2. Cellular uptake study of DOX-ACPP-DMA and DOX-ACPP-SA at pH 6.8 and 7.4 after incubation for 1 h with HeLa cells by CLSM (A) and flow cytometry (B and C). Blank (blue and red); cellular uptake of DOX-ACPP-SA at pH 7.4 (yellow) and 6.8 (purple); cellular uptake of DOX-ACPP-DMA at pH 7.4 (green) and 6.8 (black).

release would be triggered effectively by the intracellular protease for tumor treatment (Scheme 1C).

3.2. pH-Triggered Hydrolysis and Charge Reversion. In Figure 1A, at pH 6.8, with the rapid hydrolysis of the amides, the zeta potential of DOX-ACPP-DMA increased significantly and became positive in 15 min. After 4 h, it increased to nearly 15 mV. Whereas at pH 7.4, the zeta potential of DOX-ACPP-DMA was −21.3 mV and subsequently increased slowly to <2 mV, which was consistent with the finding reported in the literature.[23] Given the fact that cell membranes are usually negatively charged, the conjugate with high zeta potential would improve its internalization to cells. By contrast, the conjugate with low zeta potential would inhibit its interaction with cell membranes. Under an acidic tumor microenvironment, DOX-ACPP-DMA would be activated quickly for fast cellular uptake by tumor cells. However, at physiological pH 7.4, it remained inactive and exhibited weak interaction with normal cells.

Furthermore, after the DMA was replaced by SA, DOX-ACPP-SA continued to have quite a low zeta potential (approximately −21 mV) at either pH 7.4 or 6.8 after 4 h, suggesting that DOX-ACPP-DMA had the property of charge conversion under an acidic environment but not DOX-ACPP-SA. As a control, zeta potential changes of DOX-ACPP were also measured at pH 7.4 and 6.8 (Figure S9, SI). As expected, at either pH 7.4 or 6.8, the zeta potentials of DOX-ACPP were very stable after 4 h, and the difference at different pH values was quite modest. The obvious zeta potential difference between DOX-ACPP and DOX-ACPP-DMA at different pH also illustrates that DOX-ACPP-DMA truly has the property of charge conversion under an acidic environment, whereas DOX-ACPP does not.

For the acid-triggered degradation of DMA in DOX-ACPP-DMA to be further verified, the hydrolysis of DMA was monitored by the fluorescamine method (Figure S10, SI). The hydrolysis of DMA rapidly approached 60% within 30 min at pH 6.8 and further increased to >90% after 4 h. However, at pH 7.4, the hydrolysis profile increased slowly to reach a plateau of only 40% DMA release after 4 h. These results were coincident with the zeta potential changes in Figure 1A, demonstrating a desirable acid-triggered detachment of DMA as the shielding group.

3.3. In Vitro Enzymatic Release of DOX. For the successful released of the conjugated DOX to be confirmed, cathepsin B, a kind of protease, was used to hydrolyze the peptide bonds. As demonstrated in Figure 1B, there was a sudden release in the presence of cathepsin B with ∼70% of DOX released within 10 h. By contrast, <20% of DOX was released after 96 h without cathepsin B. Obviously, the conjugated DOX could be released successfully as the amide bond was hydrolyzed by cathepsin B, which is present in tumor cells. Here, it should be noted that a report found no obvious

DOI: 10.1021/acsami.5b04517
ACS Appl. Mater. Interfaces 2015, 7, 16061−16069

effect difference after coupling a small molecule to DOX,[36,37] and the conjugated DOX released from the prodrug would play a same role in tumor treatment as free DOX.

3.4. Cellular Uptake. Further demonstrating whether DOX-ACPP-DMA could be efficiently internalized under the tumor extracellular environment (pH_e) required investigating cellular uptake behaviors at pH 7.4 and 6.8 by CLSM and flow cytometry. DOX-ACPP-DMA was cultured with HeLa cells for 1 h at 37 °C. As shown in Figure 2A, DOX-ACPP-DMA showed an obvious internalizing behavior and concentrated distribution in the cytoplasm at pH 6.8, which was barely observed in the identical cells at pH 7.4. Furthermore, as the control, DOX-ACPP-SA was also cultured with HeLa cells by the same method and almost no fluorescence was found in the cells at either pH 6.8 or 7.4.

The cellular uptake of DOX-ACPP-DMA and DOX-ACPP-SA were also measured by flow cytometry (Figure 2B and C), which showed a similar phenomenon to that in Figure 2A. Cells could uptake DOX-ACPP-DMA more efficiently at pH 6.8 than 7.4 but could hardly uptake DOX-ACPP-SA at either pH 6.8 or 7.4. These results were coincident with the zeta potential changes in Figure 1A, implying that the rapid hydrolysis of DMA led to charge reversal and activated the pristine functioning CPP for improved cellular uptake by tumor cells.

For the influence of DOX-ACPP-DMA on normal cells to be understood, DOX-ACPP-DMA was cultured with COS7 cells for 1 h at 37 °C. Cellular uptake behaviors were investigated at pH 7.4 and 6.8 by CLSM and flow cytometry. As shown in Figure 3, there was little difference compared with HeLa cells, demonstrating that, at pH 7.4, the cell-penetrating function of R_8 was effectively blocked to inhibit DOX-ACPP-DMA's internalization by normal cells, which would be useful for the alleviation of side effects.

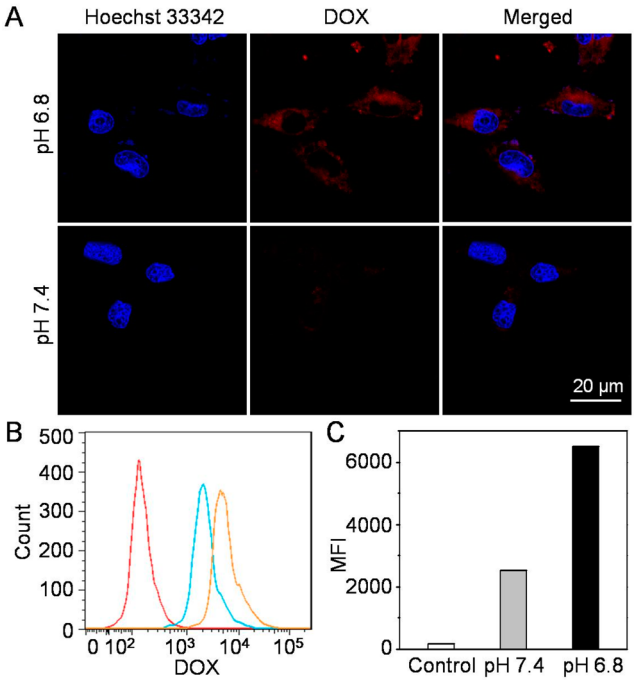

Figure 3. Cellular uptake study of DOX-ACPP-DMA at pH 6.8 and 7.4 after incubation for 1 h with COS7 cells by CLSM (A) and flow cytometry (B and C). Blank (red); cellular uptake of DOX-ACPP-DMA at pH 7.4 (blue) and 6.8 (yellow).

For the efficient release of DOX from the conjugated prodrug to be further proven, HeLa cells were incubated with DOX-ACPP-DMA at pH 6.8 for different time intervals. As shown in Figure 4, after incubation for 2 h, DOX-ACPP-DMA

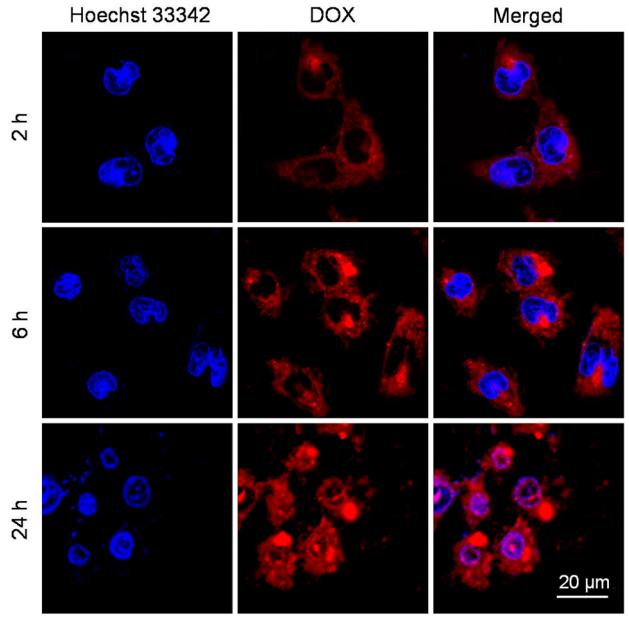

Figure 4. CLSM images of HeLa cells treated with DOX-ACPP-DMA at pH 6.8 for 2, 6, and 24 h.

was concentrated in the cytoplasm with rare DOX observed in the nuclei. However, after incubation from 6 to 24 h, visibly increased DOX was observed in the cell nuclei, implying the efficient release of DOX from the conjugated prodrug.

3.5. Cytotoxicity Assay. The in vitro cytotoxicity of DOX-ACPP-DMA against HeLa and COS7 cells was evaluated using the MTT assay. As exhibited in Figure 5A, in either HeLa or COS7 cells, the DOX-ACPP-DMA conjugate displayed lower cell viability at pH 6.8 than pH 7.4. With increased concentration of DOX, the cell viability decreased significantly at pH 6.8. The result was also consistent with the zeta potential changes and cellular uptake, reflecting the specific response of DOX-ACPP-DMA to the tumor extracellular environment (pH_e 6.8).

As the controls, ACPP, free DOX, and DOX-ACPP were incubated with HeLa cells at pH 7.4. As demonstrated in Figure 5B, ACPP had almost no toxicity because of its good cell compatibility. After being conjugated with DOX, the conjugate showed a distinct dose-dependent cytotoxicity. The same results were also found when incubated with HeLa cells at pH 6.8 (Figure S11, SI). DOX reflected a high toxicity at low doses because it was readily transported into cells by passive diffusion. At pH 7.4, compared with free DOX and DOX-ACPP, DOX-ACPP-DMA showed a very low cytotoxicity, which implied that it would generate negligible damage to normal tissues. On the contrary, its high cytotoxicity at pH 6.8 also demonstrated that it was effective for treating tumors. Furthermore, the in vitro cytotoxicities of ACPP, DOX-ACPP, and free DOX against COS7 cells were evaluated at pH 7.4 (Figure S12, SI) and are also highly consistent with their in vitro cell viability assay results in HeLa cells because of their nonselectivity.

3.6. In Vivo Antitumor Evaluation. The in vivo antitumor evaluation was demonstrated against hepatic tumor H22 cells in

DOI: 10.1021/acsami.5b04517
ACS Appl. Mater. Interfaces 2015, 7, 16061−16069

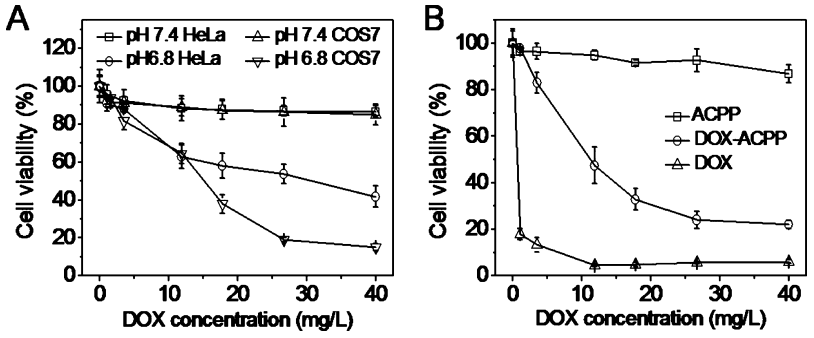

Figure 5. (A) In vitro cell viability assay of DOX-ACPP-DMA in HeLa and COS7 cells at pH 7.4 and 6.8 for 48 h. (B) In vitro cell viability assay of ACPP, DOX-ACPP, and free DOX in HeLa cells at pH 7.4 for 48 h.

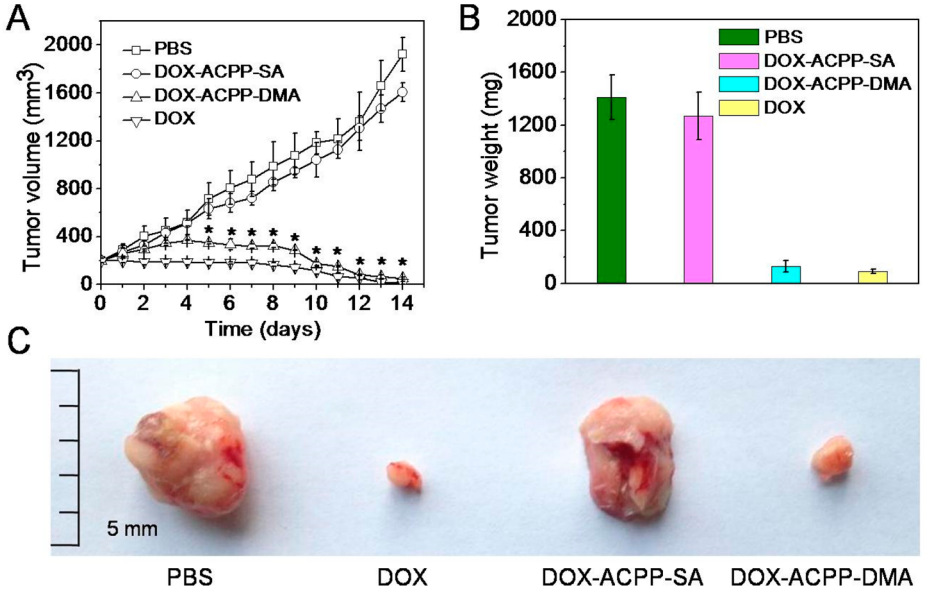

Figure 6. In vivo antitumor effects after different treatments on H22 xenografted mice. (A) Tumor volume changes after treatment with PBS, DOX-ACPP-SA, DOX-ACPP-DMA, and free DOX, respectively. Weight (B) and photo images (C) of the tumor separated from mice after various treatments for 14 days. The data are presented as the mean ± SD (n = 5). *P < 0.05 DOX-ACPP-SA vs DOX-ACPP-DMA.

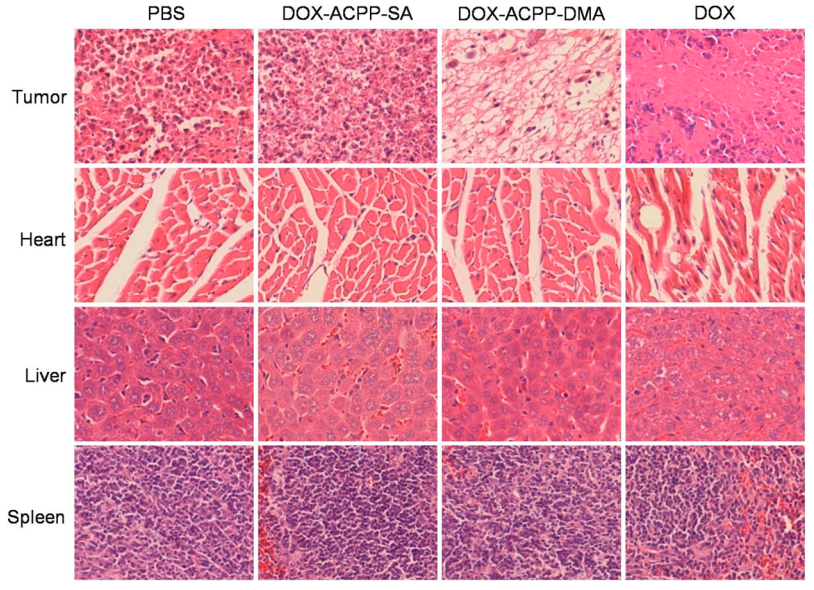

Figure 7. Histological section of the tumor, heart, liver, and spleen tissues of mice after treatment with PBS, DOX-ACPP-SA, DOX-ACPP-DMA, and free DOX, respectively. Hematoxylin-eosin staining; 200× magnification.

DOI: 10.1021/acsami.5b04517
ACS Appl. Mater. Interfaces 2015, 7, 16061−16069

female KM mice. As shown in Figure 6A, without any treatment, the tumor xenograft volume of the PBS group quickly increased to nearly 2000 mm^3 after 14 days. However, when treated with DOX-ACPP-DMA, the tumor initially increased slowly and then decreased sharply. After 14 days, the tumor xenograft volume decreased to ~50 mm^3, suggesting that DOX-ACPP-DMA had significantly inhibited tumor growth. Meanwhile, as a control, the antitumor activity of DOX-ACPP-SA was evaluated. Within the same time frame, the tumor xenograft volume increased to ~1600 mm^3. There was a significant difference between the DOX-ACPP-DMA and DOX-ACPP-SA groups (statistical P values <0.05). This finding was also observed in the tumor weights of these three groups (Figure 6B). After treatment for 14 days, the tumor weight of the DOX-ACPP-DMA group was only ~130 mg, which was significantly lower than those of the PBS (1410 mg) and DOX-ACPP-SA groups (1267 mg). A similar difference emerged for the tumor separated from mice after treatment for 14 days (Figure 6C). In addition, although free DOX had the same antitumor effect (tumor volume of 14 mm^3, tumor weight of 90 mg) as DOX-ACPP-DMA, it also caused serious side effects that influenced the growth of the mice that were not found in other groups (data not shown).

3.7. Histological Examination. For the antitumor activity of DOX-ACPP-DMA to be further analyzed, histological examination was used to observe the morphology of cells in major organs and the tumors. As presented in Figure 7, tumors treated with PBS or DOX-ACPP-SA were mainly filled with abundant tumor cells without obvious damage. By contrast, there were a large number of apoptotic or necrosis cells without nuclei in tumor tissues after treatment with DOX-ACPP-DMA or free DOX. Clearly, DOX-ACPP-DMA displayed a significant antitumor effect, and it even had an equivalent effect with free DOX. Compared with free DOX, DOX-ACPP-DMA was specific to tumor cells without obvious subacute toxicity to the heart or liver. As shown in both DOX-ACPP-SA and DOX-ACPP-DMA groups, the morphologies of the cells in the heart and liver were analogous to those of the cells in the PBS group, indicating no apparent toxicity to heart and liver tissues. Nevertheless, in the group with free DOX, there were obvious myocardial damage phenomena, such as extensive irregular arrangement and shrinkage of the cells. Furthermore, severe damage through apoptosis and nuclear shrinkage was also observed in liver tissues of the DOX group. Noted here, no significant toxicity was found in the spleen tissue of either group. In all, DOX-ACPP-DMA exhibited significant inhibition of tumor growth in vivo with significantly reduced side effects.

4. CONCLUSIONS

In conclusion, an ACPP-conjugated prodrug, DOX-ACPP-DMA, with the property of charge conversion, was designed for tumor targeted drug delivery. Amidization of the ACPP's lysine residues could efficiently block its cell penetration function by intramolecular electrostatic attraction. Once the amidized ACPP reached the tumor tissue, the amides were quickly hydrolyzed, activating the pristine functioning CPP for fast cellular uptake by tumor cells. After the internalization, the conjugated DOX was released effectively by intracellular protease (cathepsin B) for tumor treatment. Taking advantage of the pH sensitivity, CPP mediated membrane penetration and intracellular protease-induced drug release; the peptidic prodrug exhibited great superiority in tumor therapy both in vitro and in vivo with reduced side effects. This ACPP-conjugated prodrug, activated by the acidic microenvironment of the tumor, could have great potential for tumor therapy.

■ ASSOCIATED CONTENT

Supporting Information

MALDI-TOF-MS and HPLC profiles of ACPP and DOX-ACPP,

ESI-MS and HPLC profiles of DOX-SMP, NMR spectrum and HPLC profile of DOX-ACPP-DMA, zeta potential and hydrolysis effects of DOX-ACPP, and cell viability of HeLa and COS7 cells exposed to ACPP, DOX, and free DOX. The Supporting Information is available free of charge on the ACS Publications website at DOI: 10.1021/acsami.5b04517.

■ AUTHOR INFORMATION

Corresponding Author

*Tel. & Fax: 86-27-68754509. E-mail address: xz-zhang@whu.edu.cn.

Notes

The authors declare no competing financial interest.

■ ACKNOWLEDGMENTS

We are grateful for the financial support of the Natural Science Foundation of Hubei Province of China (2014CFB696 and 2013CFA003), National Natural Science Foundation of China (21074098), and National Key Basic Research Program of China (2011CB606202).

■ REFERENCES

(1) Jones, B. Tumor Genetics: Evaluating Oncogene Cooperativities. *Nat. Rev. Genet.* **2012**, *13*, 598.

(2) Maksimenko, A.; Dosio, F.; Mougin, J.; Ferrero, A.; Wack, S.; Reddy, L. H.; Weyn, A.; Lepeltier, E.; Bourgaux, C.; Stella, B.; Cattel, L.; Couvreur, P. A Unique Squalenoylated and Nonpegylated Doxorubicin Nanomedicine with Systemic Long-Circulating Properties and Anticancer Activity. *Proc. Natl. Acad. Sci. U. S. A.* **2014**, *111*, 217−226.

(3) Cai, T. T.; Lei, Q.; Yang, B.; Jia, H. Z.; Cheng, H.; Liu, L. H.; Zeng, X.; Feng, J.; Zhuo, R. X.; Zhang, X. Z. Utilization of H-Bond Interaction of Nucleobase Uralic with Antitumor Methotrexate to Design Drug Carrier with Ultrahigh Loading Efficiency and pH-Responsive Drug Release. *Regen. Biomater.* **2014**, *1*, 27−35.

(4) Wu, H.; Zhu, L.; Torchilin, V. P. pH-Sensitive Poly(histidine)-PEG/DSPE-PEG Co-Polymer Micelles for Cytosolic Drug Delivery. *Biomaterials* **2013**, *34*, 1213−1222.

(5) Mahato, R.; Tai, W.; Cheng, K. Prodrug for Improving Tumor Target Ability and Efficiency. *Adv. Drug Delivery Rev.* **2011**, *63*, 659−670.

(6) Giang, I.; Boland, E. L.; Poon, G. M. K. Prodrug Application for Targeted Cancer Therapy. *AAPS J.* **2014**, *16*, 899−913.

(7) Jiang, T.; Li, Y. M.; Lv, Y.; Cheng, Y. J.; He, F.; Zhuo, R. X. Amphipilic Polycarbonate Conjugates of Doxorubicin with pH-Sensitive Hydrazone Linker for Controlled Release. *Colloids Surf., B* **2013**, *111*, 542−548.

(8) Li, Y.; Liu, R. Y.; Yang, J.; Ma, G. H.; Zhang, Z. Z.; Zhang, X. Dual Sensitive and Temporally Controlled Camptothecin Prodrug Liposomes Codelivery of siRNA for High Efficiency Tumor Therapy. *Biomaterials* **2014**, *35*, 9731−9745.

(9) Hochdorffer, K.; Ajaj, K. A.; Obodozie, C. S.; Kratz, F. Development of Novel Bisphosphonate Prodrugs of Doxorubicin for Targeting Bone Metastases That Are Cleaved pH Dependently or by Cathepsin B: Synthesis, Cleavage Properties, and Binding Properties to Hydroxyapatite as Well as Bone Matrix. *J. Med. Chem.* **2012**, *55*, 7502−7515.

(10) Toriyabe, N.; Hayashi, Y.; Harashima, H. The Transfection Activity of R8-Modified Nanoparticles and siRNA Condensation

DOI: 10.1021/acsami.5b04517
ACS Appl. Mater. Interfaces 2015, 7, 16061−16069

Using pH Sensitive Stearylated- Octahistidine. *Biomaterials* **2013**, *34*, 1337−1343.
(11) Yang, Y. F.; Yang, Y.; Xie, X. Y.; Cai, X. S.; Zhang, H.; Gong, W.; Wang, Z. Y.; Mei, X. G. PEGylated Liposomes with NGR Ligand and Heat-Activable Cell-Penetrating Peptide-Doxorubicin Conjugate for Tumor-Specific Therapy. *Biomaterials* **2014**, *35*, 4368−4381.
(12) Ookubo, N.; Michiue, H.; Kitamatsu, M.; Kamamura, M.; Nishiki, T.; Matsui, H. The Transdermal Inhibition of Melanogenesis by A Cell-Membrane-Permeable Peptide Delivery System Based on Poly-Arginine. *Biomaterials* **2014**, *35*, 4508−4516.
(13) Ye, J. X.; Shin, M. C.; Liang, Q. L.; He, H. N.; Yang, V. C. 15 Years of ATTEMPTS: A Macromolecular Drug Delivery System Based on the CPP-Mediated Intracellular Drug Delivery and Antibody Targeting. *J. Controlled Release* **2015**, *205*, 58−69.
(14) Jiang, T.; Olson, E. S.; Nguyen, Q. T.; Roy, M.; Jennings, P. A.; Tsien, R. Y. Tumor Imaging by Means of Proteolytic Activation of Cell-Penetrating Peptides. *Proc. Natl. Acad. Sci. U. S. A.* **2004**, *101*, 17867−17872.
(15) Olson, E. S.; Jiang, T.; Aguilera, T. A.; Nguyen, Q. T.; Ellies, L. G.; Scadeng, M.; Tsien, R. Y. Activatable Cell Penetrating Peptides Linked to Nanoparticles as Dual Probes for In Vivo Fluorescence and MR Imaging of Proteases. *Proc. Natl. Acad. Sci. U. S. A.* **2010**, *107*, 4311−4316.
(16) Nguyen, Q. T.; Olson, E. S.; Aguilera, T. A.; Jiang, T.; Scadeng, M.; Ellies, L. G.; Tsien, R. Y. Surgery with Molecular Fluorescence Imaging Using Activatable Cell-Penetrating Peptides Decreases Residual Cancer and Improves Survival. *Proc. Natl. Acad. Sci. U. S. A.* **2010**, *107*, 4317−4322.
(17) Jin, E. L.; Zhang, B.; Sun, X. R.; Zhou, Z. X.; Ma, X. P.; Sun, Q. H.; Tang, J. B.; Shen, Y. Q.; Van Kirk, E.; Murdoch, W. J.; Radosz, M. Acid-Active Cell-Penetrating Peptides for In Vivo Tumor-Targeted Drug Delivery. *J. Am. Chem. Soc.* **2013**, *135*, 933−940.
(18) van Duijnhoven, S. M. J.; Robillard, M. S.; Nicolay, K.; Grull, H. Tumor Targeting of MMP-2/9 Activatable Cell-Penetrating Imaging Probes Is Caused by Tumor-Independent Activation. *J. Nucl. Med.* **2011**, *52*, 279−286.
(19) Kluger, R.; Lam, C. H. External General Base Catalysis and General Acid Catalysis in Reactions of Norbornenylanilic Acids. *J. Am. Chem. Soc.* **1978**, *100*, 2191−2197.
(20) Lee, Y.; Fukushima, S.; Bae, Y.; Hiki, S.; Ishii, T.; Kataoka, K. A Protein Nanocarrier from Charge-Conversion Polymer in Response to Endosomal pH. *J. Am. Chem. Soc.* **2007**, *129*, 5362−5363.
(21) Lee, Y.; Miyata, K.; Oba, M.; Ishii, T.; Fukushima, S.; Han, M.; Koyama, H.; Nishiyama, N.; Kataoka, K. Charge-Conversion Ternary Polyplex with Endosome Disruption Moiety: A Technique for Efficient and Safe Gene Delivery. *Angew. Chem., Int. Ed.* **2008**, *47*, 5163−5166.
(22) Zhou, Z. X.; Shen, Y. Q.; Tang, J. B.; Fan, M. H.; Kirk, E. A V.; Murdoch, W. J.; Radosz, M. Charge-Reversal Drug Conjugate for Targeted Cancer Cell Nuclear Drug Delivery. *Adv. Funct. Mater.* **2009**, *19*, 3580−3589.
(23) Du, J. Z.; Du, X. J.; Mao, C. Q.; Wang, J. Tailor-Made Dual pH-Sensitive Polymer−Doxorubicin Nanoparticles for Efficient Anticancer Drug Delivery. *J. Am. Chem. Soc.* **2011**, *133*, 17560−17563.
(24) Li, L.; Yang, Q. Q.; Zhou, Z.; Zhong, J. J.; Huang, Y. Doxorubicin-Loaded, Charge Reversible, Folate Modified HPMA Copolymer Conjugates for Active Cancer Cell Targeting. *Biomaterials* **2014**, *35*, 5171−5187.
(25) Ding, D.; Kwok, R. T. K.; Yuan, Y. Y.; Feng, G. X.; Tang, B. Z.; Liu, B. A Fluorescent Light-up Nanoparticle Probe with Aggregation-Induced Emission Characteristics and Tumor-Acidity Responsiveness for Targeted Imaging and Selective suppression of Cancer Cells. *Mater. Horiz.* **2015**, *2*, 100−105.
(26) Jiang, L.; Li, L.; He, X. D.; Yi, Q. Y.; He, B.; Cao, J.; Pan, W. S.; Gu, Z. W. Overcoming Drug-Resistant Lung Cancer by Paclitaxel Loaded Dual-Functional Liposomes with Mitochondria Targeting and pH-Response. *Biomaterials* **2015**, *52*, 126−139.
(27) Dong, C. H.; Liu, Z. Y.; Zhang, L.; Guo, W. S.; Li, X.; Liu, J. Q.; Wang, H. J.; Chang, J. pHe-Induced Charge-Reversible NIR Fluorescence Nanoprobe for Tumor-Specific Imaging. *ACS Appl. Mater. Interfaces* **2015**, *7*, 7566−7575.
(28) Podgorski, I.; Sloane, B. F. Cathepsin B and Its Role(s) in Cancer Progression. *Biochem. Soc. Symp.* **2003**, *70*, 263−276.
(29) Zhong, Y. J.; Shao, L. H.; Li, Y. Cathepsin B-Cleavable Doxorubicin Prodrugs for Targeted Cancer Therapy (Review). *Int. J. Oncol.* **2013**, *42*, 373−383.
(30) Schmid, B.; Chung, D. E.; Warnecke, A.; Fichtner, I.; Kratz, F. Albumin-Binding Prodrugs of Camptothecin and Doxorubicin with An Ala-Leu-Ala-Leu-Linker That Are Cleaved by Cathepsin B: Synthesis and Antitumor Efficacy. *Bioconjugate Chem.* **2007**, *18*, 702−716.
(31) Abu Ajaj, K.; Graeser, R.; Fichtner, I.; Kratz, F. In Vitro and In Vivo Study of An Albumin-Binding Prodrug of Doxorubicin That Is Cleaved by Cathepsin B. *Cancer Chemother. Pharmacol.* **2009**, *64*, 413−418.
(32) Han, K.; Chen, S.; Chen, W. H.; Lei, Q.; Liu, Y.; Zhuo, R. X.; Zhang, X. Z. Synergistic Gene and Drug Tumor Therapy Using A Chimeric Peptide. *Biomaterials* **2013**, *34*, 4680−4689.
(33) Oh, N. M.; Kwag, D. S.; Oh, K. T.; Youn, Y. S.; Lee, E. S. Electrostatic Charge Coversion Processes in Engineered Tumor-Identifying Polypeptides for Targeted Chemotherapy. *Biomaterials* **2012**, *33*, 1884−1893.
(34) Li, L.; Yang, Q. Q.; Zhou, Z.; Zhong, J. J.; Huang, Y. Doxorubicin-Loaded, Charge Reversible, Folate Modified HPMA Copolymer Conjugates for Active Cancer Cell Targeting. *Biomaterials* **2014**, *35*, 5171−5187.
(35) Chen, J. X.; Xu, X. D.; Chen, W. H.; Zhang, X. Z. Multi-Functional Envelope-Type Nanoparticles Assembled from Amphiphilic Peptidic Prodrug with Improved Anti-Tumor Activity. *ACS Appl. Mater. Interfaces* **2014**, *6*, 593−598.
(36) Santra, S.; Kaittanis, C.; Santiesteban, O. J.; Perez, J. M. Cell-Specific, Activatable, and Theranostic Prodrug for Dual-Targeted Cancer Imaging and Therapy. *J. Am. Chem. Soc.* **2011**, *133*, 16680−16688.
(37) Yuan, Y. Y.; Liu, J.; Liu, B. Conjugated-Polyelectrolyte-Based Polyprodrug: Targeted and Image-Guided Photodynamic and Chemotherapy with On-Demand Drug Release upon Irradiation with a Single Light Source. *Angew. Chem., Int. Ed.* **2014**, *53*, 7163−7168.

DOI: 10.1021/acsami.5b04517
ACS Appl. Mater. Interfaces 2015, 7, 16061−16069